Scientia Iranica C (2017) 24(6), 3002–3013

SCIENTIA IRANICA

Sharif University of Technology
Scientia Iranica
Transactions C: Chemistry and Chemical Engineering
www.scientiairanica.com

Synthesis of N^{α}-protected formamides from amino acids using MgO nano catalyst: Study of molecular docking and antibacterial activity

M. Raghavendra[a], H.S. Lalithamba[a,*], B.S. Sharath[b] and H. Rajanaika[c]

a. *Department of Chemistry, Siddaganga Institute of Technology, Tumakuru - 572 103, Karnataka, India.*
b. *Department of PG Studies & Research in Biotechnology & Bioinformatics, Kuvempu University, Shankaraghatta - 577451, Shimoga, Karnataka, India.*
c. *Department of Studies and Research in Environmental Science, Tumkur University, Tumakuru - 572 103, Karnataka, India.*

Received 23 January 2017; received in revised form 2 April 2017; accepted 25 September 2017

KEYWORDS
Formamides;
Nano MgO;
Curtius rearrangement;
Molecular docking;
Antibacterial activity.

Abstract. Green synthesis of nano MgO particles and their application in the formylation of isocyanates of *N*-Fmoc/Cbz/Boc protected amino acids were reported. Nano magnesium oxide catalysed reaction of isocyanate with 96% formic acid was established to obtain formamides. For this, the carboxyl group of protected amino acids was activated via mixed anhydride method and treated with NaN_3. The formed azides were converted into their isocyanates through Curtius rearrangement and treated with HCOOH and catalytic amount of nano MgO. The advantages of this method were being remarkably simple and attaining economically low-cost nano metal oxide under milder reaction conditions. Most importantly, MgO could be easily separated and other basic impurities were removed through a simple work-up. This protocol showed high efficiency in catalysing the transformation in a greener fashion. The molecular docking study of the synthesized compounds was performed against the macromolecules sortase-A and glucosamine 6-phosphate synthase to understand the binding interactions. The results of *in vitro* antibacterial activities of the synthesized compounds were supported by docking analysis.

1. Introduction

Nanoparticles have proved to be useful to chemists in laboratory and industry, owing to the good activation of adsorbed compounds and enhancement of the reaction rate, selectivity, easier work-up, and eco-friendly reaction conditions [1-3]. Nano-structured materials, compared to micron-sized materials, possess the unique characteristic of large specific surface areas, making a large fraction of atoms available for chemical reaction. Nano MgO serves as catalyst as well as reagent due to its improved physical and chemical properties in many syntheses; it has low-cost production, minimal side product and high-level chemoselectivity, and environmental compatibility. Hence, it has many applications such as in deflouridation of water purification, adsorbing, medical sciences, catalysis, additives to heavy fuel oils, lithium ion batteries, etc. [4-7]. Different methods are available in the literature to prepare MgO Nps, e.g., sonochemical method, precipitation, solvothermal method, microwave irradiations,

*. *Corresponding author. Fax: 0816 2282994*
E-mail addresses: raghu1289@hotmail.com (M. Raghavendra); lalithambasit@yahoo.co.in (H.S. Lalithamba); sharathbio123@gmail.com (B.S. Sharath); rajanaika@tumkuruniversity.ac.in (H. Rajanaika)

doi: 10.24200/sci.2017.4491

carbothermic reduction, solid-state reaction, thermal decomposition of precursor, etc. [8-13]. Chemical methods of synthesis lead to the presence of some toxic chemicals absorbed on the surface, which may cause harmful effects in medical applications. Recently, green synthesis of different nanoparticles by plants such as Neem, Alfalfas, Papaya, Black Tea, and Tamarind have been reported [14-18]. In this paper, we report the facile green synthesis of MgO Nps via solution combustion method using garcinia gummi-gutta seed extract. This is one of garcinia species and belongs to a family Clusiaceae, which thrives best in the evergreen forests of Konkan, coastal and southern parts of Kerala, and Western Ghats up to 180 m in the Nilgiris. It is commonly grown as miscellaneous stray spice tree in the homesteads of coastal saline belt of Kerala, Karnataka, and Sri Lanka. It produces fleshy fruits, which contain about 30-40% oil. The skin of the fruit, which contains large amount of a natural substance called hydroxycitric acid, the active ingredient in garcinia gummi-gutta extract, helps in reducing body weight [19-21].

Further, the present study focuses on the use of nano MgO for the synthesis of N^{α}-protected amino acid derived formamides. Formamide is a highly polar molecule, called methanamide, and an amide bond widely prevalent in both naturally occurring and synthetic compounds. N^{α}-formyl compounds have been extensively used in organic synthesis as protecting group for amines [22,23]. They are also used for synthesis of medicinally important heterocycles [24]. Formamides are the smallest units and useful intermediates for the synthesis of pharmaceutically valuable compounds and chemotherapeutic agents, which have attracted the attention of biologists and biochemists [25,26]. Structurally modified molecules include monomethylated amines, isocyanides, and formamidines with formamide skeleton and are of considerable interest in the field of organic chemistry [27-30]. They have also been employed as Lewis bases in several organic transformations and used as a co-solvent (additive) for catalysing the sol-gel reactions and for the evolution of chemical structure [31,32].

Generally, formamides are synthesized by the reaction of isocyanate and formic acid in the presence of DMAP (4-(dimethylamino)pyridine) [33]. Alternatively, few more formylating reagents like acetic formic anhydride, ammonium formate, activated formic esters, chloral, imidazole-DMF and catalysts VB_1, Zn metal, ZnO with formic acid may be used [34-38]. Many other useful catalysts such as aqueous formaldehyde-iridium, CeO_2-formic acid, imidazolium-based ionic liquid CO_2, and stearic acid-nano-sulphated TiO_2 have been reported [39-43]. However, many of these procedures suffer from the difficulties such as high toxicity, expensive reagents, prolonged reaction time, and issues associated with impurities, which need further purification and require special care. Therefore, using a convenient reagent is necessary for the synthesis of stable formamides in terms of operational simplicity and economic viability.

2. Results and discussion

N-formamides (N-formylated *gem*-diamines) from protected amino acids were meticulously synthesized according to the protocol sketched in Scheme 1. The proposed structures of synthesized compounds were characterized through spectral analysis and, then, processed further for the antibacterial activity evaluation using two bacterial strains. The general reaction conditions and structure characterization are provided in the experimental section.

2.1. Chemistry

In this context, we proceeded with the reaction of Fmoc/Cbz/Boc-amino-isocyanates with formic acid in the presence of nano MgO. The synthetic utilities of N^{α}-protected amino isocyanates in the preparation of peptidomimetics like peptidylureas have been described in the literature [44]. Herein, we present a useful application of amino acid derived isocyanates in the synthesis of the N-formylated *gem*-diamines by the reaction of N-protected amino isocyanates with formic acid in the presence of nano MgO (Scheme 1). N^{α}-protected amino acid **1** was dissolved in THF (tetrahydrofuran) and its carboxyl group was activated by the addition of NMM (N-methyl morpholine) coupled with ECF (ethyl chloroformate) at -10 to -15°C. The reaction mixture was stirred for 15 minutes at the same temperature and aqueous NaN_3 was added to get acyl azide; progress of the reaction was monitored through TLC (Thin Layer Chromatography). Then, THF was evaporated in vacuum and the reaction mixture was dissolved in DCM (dichloromethane). After the simple work-up, DCM was removed under reduced pressure and the residue was dissolved in toluene due to its better compatibility under reflux condition. The

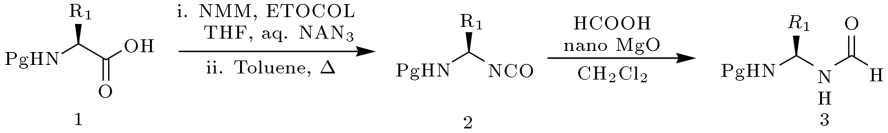

1 2 3

Scheme 1. Synthesis of N-formamides from N^{α}-amino acids. R^1, H, Alkyl, Aryl; Pg (protecting group).

Table 1. List of N^{α}-protected formamides prepared via Scheme 1.

Entry	Formamides	Yield (%)	Mp (°C)
3a	Fmoc-gVal-CO-H	84	183
3b	Fmoc-gPhe-CO-H	82	191
3c	Cbz-*g*Gly-CO-H	89	161
3d	Cbz-*g*Met-CO-H	75	159
3e	Boc-*g*Ala- CO-H	79	183
3f	Fmoc-*g*Ala-CO-H	82	178
3g	Fmoc-*g*Leu-CO-H	76	156
3h	Fmoc-*g*Pro-CO-H	75	Gum
3i	Fmoc-*g*Ile-CO-H	86	140
3j	Fmoc-*g*Try-CO-H	87	178
3k	Cbz-*g*Ser-CO-H	75	178
3l	Boc-*g*Phe-CO-H	78	178
3m	Cbz-*g*Ile-CO-H	77	147
3n	Boc-*g*Thr-CO-H	80	177
3o	Cbz-*g*Phe-CO-H	92	175

Note: The notation "*g*" in Fmoc-*g*Xaa-CO-H represents the *gem*-diamine derivative

formed azide was subject to Curtius rearrangement by means of refluxing the solution for 45 min; the resulting isocyanate **2** was immediately reacted with HCO_2H in the presence of nano MgO to afford the required *N*-formylated *gem*-diamines **3** via Scheme 1. The resulting mixture was stirred at 0°C for 4 hours until completion of the reaction (as monitored by TLC). Then, the reaction mixture was washed with citric acid, Na_2CO_3 solution, and water and, finally, purified through recrystallization using DMSO-H_2O. Using this procedure, several formamides (**3a-o**) were synthesized from N^{a}-protected amino acids as shown in the Table 1. The synthesized compounds were confirmed by their FTIR, ^{1}H NMR, ^{13}C NMR, and mass spectral studies. Product isolation in most cases was straightforward as they were precipitated in the reaction mixture. However, some of the Cbz and Boc-formamides were not precipitated and required a simple workup. The main advantages of using MgO Nps are easy handling, cost effectiveness, and minimal by-products compared to the reagent [45]. In addition, we tried the reaction in the presence of large amount of MgO (> 0.5 mmol) at room temperature, which did not affect final yield of the products and reaction rate, but < 0.5 mmol considerably decreased the percentage of formamides. The application of nano MgO for the transformation of carboxylic acid function of the *N*-protected amino acid into a formamide moiety has not been established in the literature. A reaction of such kind would lead to the generation of a formamide, forming a new type of synthons to carry out the chemical transformations analogous to the existing reactions of the *N*-formyl group.

2.2. Morphological and structural characterization of nano MgO Nps

The XRD pattern of MgO nanoparticles (Nps) obtained from solution combustion method is shown in Figure 1. The result showed that it was in cubic structure and matched Joint Committee on Powder Diffraction and Standards (JCPDS) card number 75-1525. Peaks were observed at 37°, 43°, and 62° along with miller indices values of (111), (200), and (220), respectively. As the width of the peak increased, the size of particle decreased, which showed that the present material was in nano range [46]. The average crystallite size of the MgO nanoparticle was found to be 16 nm.

FTIR spectrum of MgO Nps (Figure 2) was recorded at ambient conditions with the wavelength ranging from 400 to 4000 cm^{-1}. The peak at 426.0 cm^{-1} indicated Mg-O bond stretching, which in turn confirmed that the obtained product was mag-

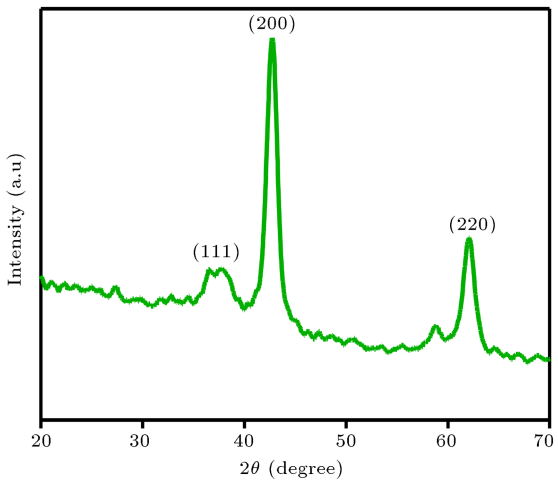

Figure 1. X-Ray powder Diffraction (XRD) patterns of the MgO nanoparticles calcined at fixed temperature.

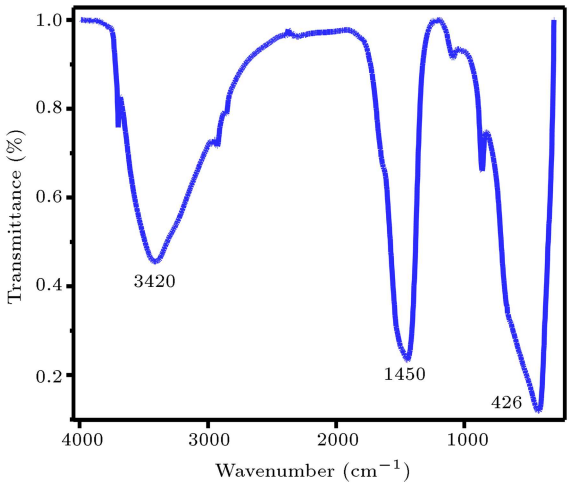

Figure 2. Fourier transform infrared (FTIR) spectrum of the MgO nanoparticles calcined at 450°C for 4 hrs.

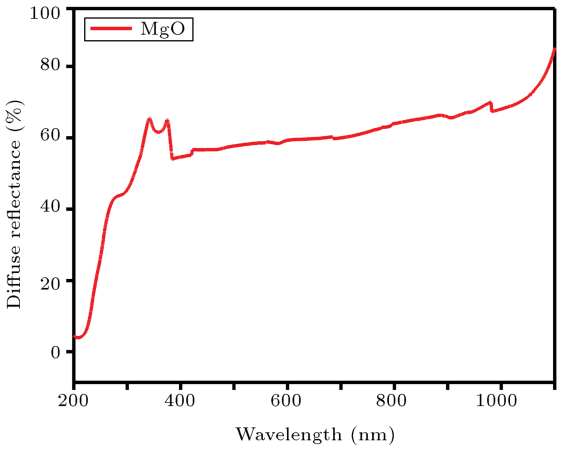

Figure 3(a). Diffuse reflectance spectrum of MgO Nps.

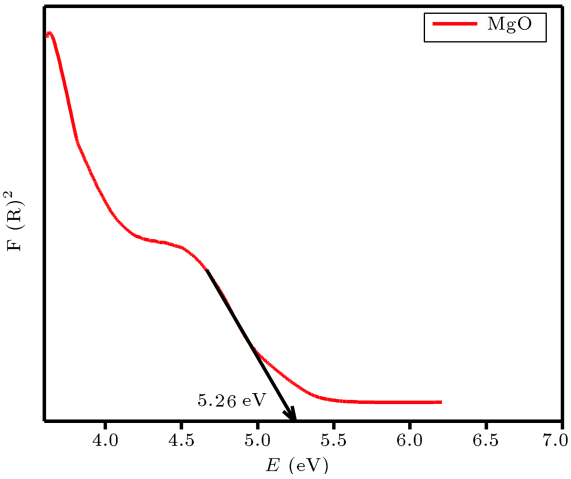

Figure 3(b). Direct band gap energy of MgO Nps.

nesium oxide. The peak observed at 1450.0 cm^{-1} and 3420.0 cm^{-1} was due to the presence of $-OH$ stretching and bending, respectively, assigned to the H_2O adsorption on the surface of metal. The metal-oxygen frequencies observed for the respective metal oxides were in accordance with the literature values [47].

Figure 3(a) depicts the Diffuse Reflectance Spectrum (DRS) of MgO Nps recorded at room temperature. It shows the characteristic absorption peak at around 400 nm; this is due to the excitonic absorption feature of MgO particles. The band gap calculated from diffused spectrum was 5.26 Ev (Figure 3(b)). However, a small difference in energy gap was observed due to synthetic method, particle size, crystallinity, morphology, etc.

Figure 4 shows the SEM images of MgO nanoparticles visualized by Scanning Electronic Microscopy. Analysing the morphology aspect of nanoparticles by studying the images indicates that the average sizes of synthesized MgO Nps ranged from 16 nm to 120 nm. This indicates that the particles have nano dimension and agglomerated shape.

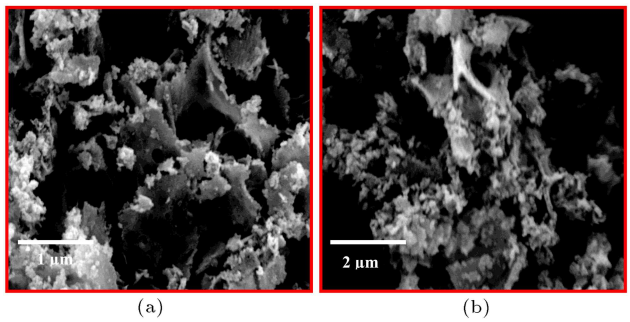

Figure 4. SEM images of MgO Nps which provide information on the size, shape, and location of the individual nanoparticles.

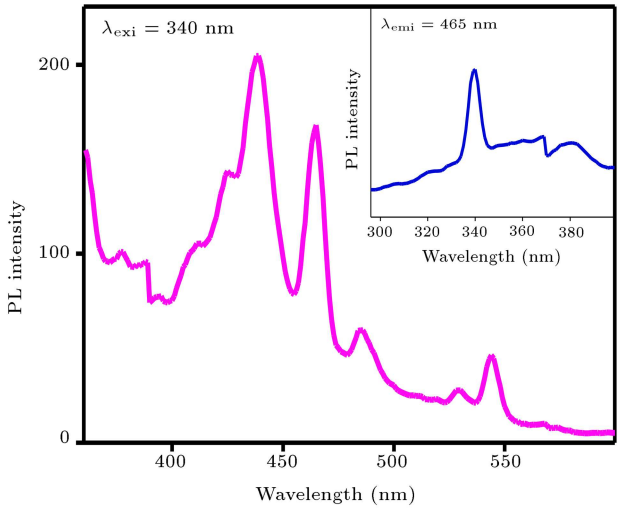

Figure 5. Photoluminescence (PL) spectra of MgO Nps. Photoluminescence study is a very sensitive analysis to measure the quality of crystal structure, presence of oxygen vacancies as common defects, and the emission mechanism.

The photoluminescence emission excitation spectrum of MgO recorded at room temperature is shown in Figure 5. In semiconductors, the recombination of the photo-generated free charge carriers leads to photoluminescence emission. The Near-Band-Edge (NBE) excitation peak at 340 nm was recorded at an emission wavelength of 465 nm. The emission spectrum monitored at 340 nm wavelength for MgO showed a broad yellow emission at 465 nm. The broad 465 nm peak was due to the transition between single charged oxygen vacancy and the photo excited holes in the valence band of the MgO material. The colour clarity of any luminescent material was expressed in terms of chromaticity coordinates, called Commission International De l'Eclairage (CIE).

2.3. Molecular docking study

Molecular docking studies have occupied a prominent place in drug discovery, which would describe the protein-ligand binding interactions and orientation of a

ligand that is bound to a particular protein. Molecular docking studies provide valuable information to predict the binding modes and the affinity between small drug molecules and the binding sites of protein present in pathogens. *In silico* molecular docking study against sortase-A [48] and glucosamine 6-phosphate synthase (macromolecules) [49] was separately performed for the synthesized ligand molecules using AutoDock/Vina.

The macromolecules with PDB ID "1T2W" and "1XFF" were downloaded from the Protein Data Bank (PDB) and edited by removing the hetero atoms. The structure of all the ligands was drawn in ACD/Chem Sketch 12.0 and optimized to 3D structures using PRODRG server. The intermediary steps, such as preparation of receptor and ligand, were completed using Autodock Tools (ADT) by assigning polar hydrogens and gasteiger charges. ADT saved the prepared file in PDBQT format. AutoDock/Vina was employed for rigid docking using protein and ligand information along with grid box properties in the configuration file. The posture with lowest binding energy cluster/complex was extracted for further analysis.

In silico docking of synthesized ligands such as Fmoc-*g*Try-CO-H (**3j**), Fmoc-*g*Ala-CO-H (**3f**), Fmoc-*g*Phe-CO-H (**3b**), Fmoc-*g*Pro-CO-H (**3h**), and Cbz-*g*Gly-CO-H (**3c**) with sortase-A and glucosamine 6-phosphate synthase provides possible anti-bacterial activity with good binding energy ranges from −5.1 kcal/mol to −8.2 kcal/mol and from −6.9 kcal/mol to −8.0 kcal/mol, respectively, by forming various interactions with the active site amino acids. Among all the synthesised compounds, Fmoc-*g*Ala-CO-H (**3f**) showed respectable interaction with glucosamine 6-phosphate synthase (Figure 6(a)), while Fmoc-*g*Try-CO-H (**3j**) showed good binding energy by exhibiting 2-H bonds with Ser116 and Pro163 with the sortase-A (Figure 7(a)); moreover, Fmoc-*g*Pro-CO-H (**3h**) with glucosamine 6-phosphate synthase showed 3-H bonds formation with the active pocket amino acids of Arg73, His77, and Thr76. Binding energy of all the ligands, depicting the docking interaction at the active pockets of sortase-A and glucosamine 6-phosphate synthase, is given in Table 2.

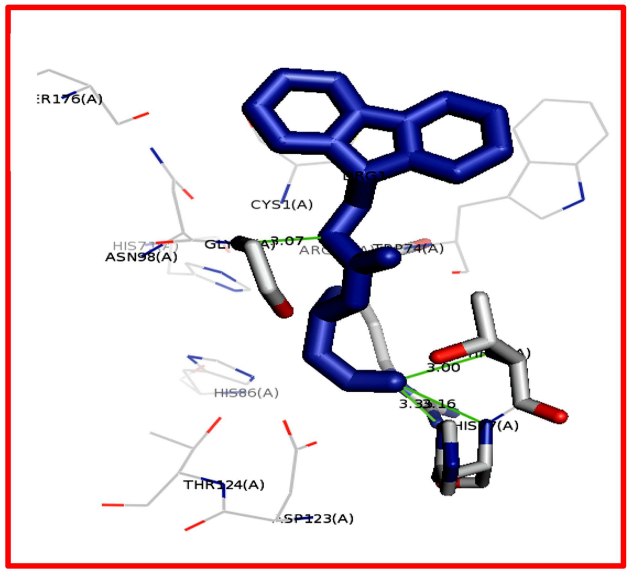

Figure 6(a). Interaction of Fmoc-*g*Ala-CO-H with glucosamine-6-phosphate synthase.

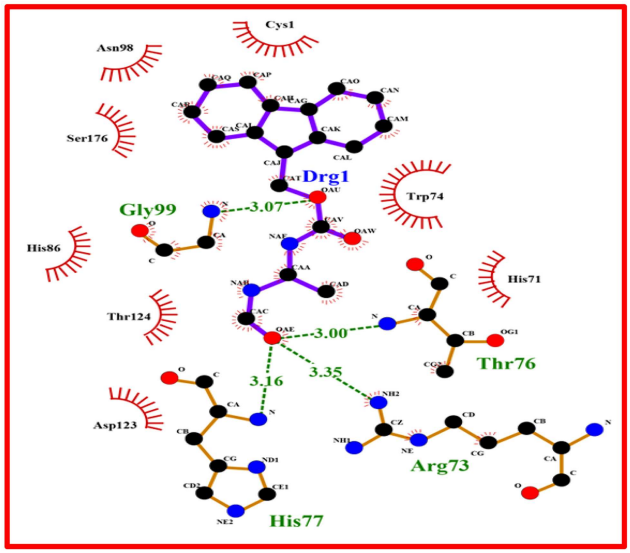

Figure 6(b). Ligplot analysis results of glucosamine-6-phosphate synthase with Fmoc-*g*Ala-CO-H. The Ligplot allows the 2D representation of multiple ligand-protein complexes in a simple and automated manner.

Molecular docking results were analysed using Ligplot and PyMol; Ligplot allows for the 2D representation of multiple protein-ligand complexes in a simple and automated manner, whereas PyMol generates 3D molecular view of protein-ligand complex [50]. Ligplot analysis results for glucosamine 6-phosphate synthase with Fmoc-*g*Ala-CO-H (**3f**) and sortase-A with Fmoc-*g*Try-CO-H (**3j**) are shown in Figures 6(b) and 7(b), respectively.

Docking results for the synthesized formamides against target proteins tabulated in Table 2 confirm that the molecules Fmoc-*g*Try-CO-H (**3j**) and Fmoc-*g*Ala-CO-H (**3f**) had large values of negative binding energy by exhibiting various interactions with the active pocket amino acids with target proteins indicating their effective binding mode.

2.4. Antibacterial activity

Antibacterial activity of synthesized formamides was screened by agar well diffusion method [51,52] against pathogenic bacterial strains such as G −ve bacteria *Escherichia coli* (NCIM-5051) and G +ve bacteria *Staphylococcus aureus* (NCIM-5022). The nutrient medium was prepared by dissolving 37.0 g of nutrient

Table 2. Docking results of the formamides with sortase-A (**1T2W**) and glucosamine 6-phosphate synthase (**1XFF**).

Ligands	Binding energy with respect to 1T2W (kcal/mol)	H-bond formation with the active pocket amino acids	Ligands	Binding energy with respect to 1XFF (kcal/mol)	H-bond formation with the active pocket amino acids
Ciprofloxacin	−6.5	—	Ciprofloxacin	−5.7	—
3b	−7.8	Arg197 (3.34)	**3h**	−7.4	Arg73; His77; Thr76 (3.20; 2.81; 2.82 & 3.02)
3j	−8.2	Ser116; Pro163 (2.79; 2.97)	**3j**	−6.9	Asn98; Cys1; Gly99 (2.96; 3.16; 3.21)
3f	−7.0	Glu105; Ser116; Asn114 (3.04; 3.03; 2.95)	**3f**	−8.0	Gly99; His77; Arg73; Thr76 (3.07; 3.16; 3.35; 3.00)
3d	−5.4	Arg197 (3.15 & 3.09)	**3c**	−7.2	Arg73; Trp74; Gly99; His77; Thr76 (3.08; 3.02; 3.22; 2.82; 2.89)
3k	−5.1	Ala104; Ala92; Trp194 (3.10; 3.01 & 3.30; 3.16)	**3k**	−6.9	His86; Arg73; Thr76; Trp74; Cys1; Gly99; His97 (3.14; 3.00; 3.11; 2.80; 2.80; 3.17 & 2.17; 2.76)

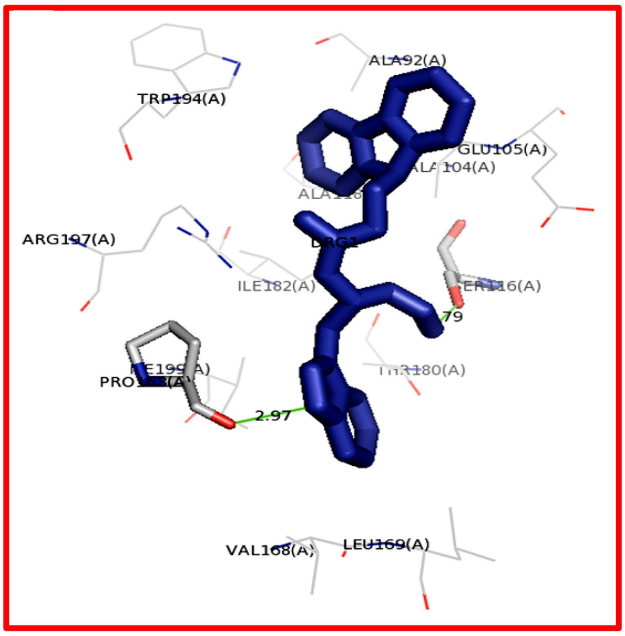

Figure 7(a). Interaction of Fmoc-*g*Try-CO-H with sortase-A.

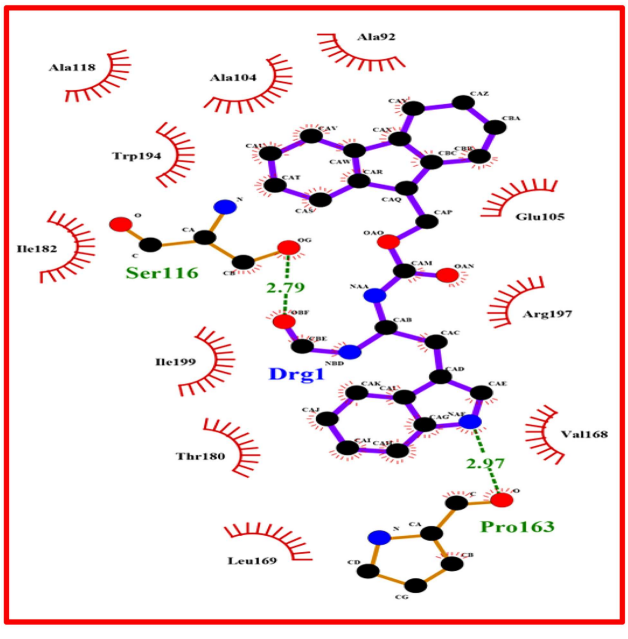

Figure 7(b). Ligplot analysis result of sortase-A with Fmoc-*g*Try-CO-H.

agar medium in 1000 ml of distilled water, adjusting the pH to 7.3 (±0.1), and subjecting the medium to sterilization in an autoclave at 121°C for 15-20 min. To prepare nutrient agar plates, 20-25 ml of sterile nutrient agar medium was poured into petri-dishes and allowed to solidify. Then, 100 μl of mature broth culture of individual pathogenic bacterial strains was spread all over the surface of agar plates using sterilized

Table 3. Antibacterial activity results of formamides with respect to Ciprofloxacin (**S**).

Samples	Treatment (concentrations)	*E. coli* (mean ± SE)	Sample	Treatment (concentrations)	*S. aureus* (Mean ± SE)
S	5μg/μL	10.13 ± 00.06	**S**	5μg/μL	11.13 ± 0.03
3k	500μg/μL	1.77 ± 0.03	**3f**	500μg/μL	1.10 ± 0.06
	1000μg/μL	3.57 ± 0.03		1000μg/μL	2.33 ± 0.03
3c	500μg/μL	1.13 ± 0.03	**3k**	500μg/μL	2.10 ± 0.06
	1000μg/μL	2.40 ± 0.06		1000μg/μL	4.13 ± 0.09
3j	500μg/μL	1.33 ± 0.03	**3b**	500μg/μL	In active
	1000μg/μL	2.73 ± 0.03		1000μg/μL	1.60 ± 0.06
3f	500μg/μL	0.53 ± 0.03	**3j**	500μg/μL	1.13 ± 0.09
	1000μg/μL	1.43 ± 0.03		1000μg/μL	2.23 ± 0.12
3h	500μg/μL	1.23 ± 0.03	**3d**	500μg/μL	In active
	1000μg/μL	3.00 ± 0.06		1000μg/μL	2.10 ± 0.06

Note: Values are the mean ± SE of inhibition zone in mm.

L-shaped glass rod. A well of about 6 mm was made in each nutrient agar plate using sterile cork borer. The test compounds were dissolved in DMSO to prepare different concentrations (500 and 1000 μg/well) used to assess the dose-dependent activity. Simultaneously, the standard antibiotic (Ciprofloxacin used as a positive control) was tested against the pathogenic bacterial strains and, then, the plates were incubated at 37°C for 36 h. After incubation, the zone of inhibition of each well was measured and the values were recorded. The experiments were carried out in triplicates with each compound and the average values were calculated for determining the antibacterial activity.

The zones of inhibition were measured with vernier callipers in mm; the values are depicted in the Table 3. These results also suggested that concentration was under the significant effect of synthesized compounds with respect to pathogenic bacterial strains. In case of *E. coli*, some formamides such as Cbz-*g*Ser-CO-H (**3k**), Fmoc-*g*Pro-CO-H (**3h**), and Fmoc-*g*Try-CO-H (**3j**) showed highly moderate zone of inhibition and compounds like Cbz-*g*Gly-CO-H (**3c**) and Fmoc-*g*Ala-CO-H (**3f**) exhibited less moderate zone of inhibitory potential. In *S. aureus* strains, the formamides such as Cbz-*g*Ser-CO-H, Fmoc-*g*Ala-CO-H, and Fmoc-*g*Trp-CO-H exhibited significant activity and less moderate zone of inhibition in the cases of Cbz-*g*Met-CO-H (**3d**) and Fmoc-*g*Phe-CO-H (**3b**). Therefore, antibacterial screening indicated that most of the compounds exhibited less antibacterial activity than the standard antibiotic did, showing no significant effect of substituent on the activity.

3. Conclusion

We developed an efficient protocol for the formylation of amino acids in the presence of a non-toxic and low-cost nano MgO powder. Solid nano metal oxides play an important role in the on-going research, especially in the field of nanotechnology. The significant advantages of the protocol were environmental friendliness, short time reaction, simple work-up, and enabling formylation of the isocyanates under mild reaction conditions. Synthesis of amino acid derived formamides involved Curtius rearrangement of amino acyl azides into corresponding isocyanates and reaction of the latter with formic acid under MgO nano catalyst. *In-silico* studies report that the formamides like Fmoc-*g*Try-CO-H and Fmoc-*g*Ala-CO-H have good affinity to the active sites of sortase-A and glucosamine 6-phosphate synthase, respectively. Based on the results obtained from molecular docking, few of the molecules with large values of negative binding energy were subject to antibacterial studies against two bacterial pathogens.

4. Experimental

4.1. General

All chemicals were purchased from Sigma-Aldrich and Merck and used without purification. The pathogenic bacterial strains were purchased from National Chemical Laboratory Pune, India. The seeds were collected from Bannergatta forest of Bangalore district, Karnataka, India. Crystalline size and phase identity of prepared products were characterized by Shimadzu X-Ray Diffractometer (PXRD-7000) using Cu-Kα radiation of wavelength $\lambda = 1.541$Å′. The absorption spectrum and band gap were measured using Lambda-35 (Parkin Elmer) spectrophotometer in the wavelength range of 200-800 nm in diffused reflectance mode. Morphological features were studied by using Hitachi-7000 Scanning Electron Microscopy, JEOL 3010 transmission electron microscope analysis. Agilent Cary Eclipse Fluorescence Spectrophotometer was used for the study of photoluminescence at room temperature. IR spectra were recorded on Bruker Alpha-T FT-IR spectrometer. ^{1}H NMR and ^{13}C NMR

spectra were recorded on a Bruker AMX 400 MHz spectrometer using $(CH_3)_4Si$ as an internal standard and DMSO (dimethylsulfoxide) as a solvent. Mass spectra were recorded on an Electrospray ionisation mass spectrometer. Melting points were taken in open capillaries and were uncorrected. TLC analysis was carried out using precoated silica gel F_{254}.

4.2. Preparation of the seed extract

The seeds were dried in moderate sunlight and, then, powdered with mesh size of 100 using mixer grinders mechanically. The powdered seeds were mixed with water in 1:10 proportion and subject to reflux for 5 hrs with stirring at 90-100°C. The filtered extract was centrifuged to remove any unwanted material. It was then concentrated and dried using heating mantle and kept in an airtight container.

4.3. Synthesis of MgO Nps (catalyst) using extract of garcinia gummi-gutta seeds

MgO Nps were prepared by combustion method, using aqueous garcinia gummi-gutta seed extract and $Mg(NO_3)_2.6H_2O$ [53]. In solution combustion method, the reaction mixture was prepared by treating garcinia gummi-gutta seed extract (fuel) and $Mg(NO_3)_2.6H_2O$ as a source of magnesium in a cylindrical petri dish and stirred for few minutes until a uniform homogenous solution was formed. This reaction mixture was kept in a pre-heated muffle furnace maintained at 450°C. MgO Nps formed within 30 min and the acquired particles were stored in air tight container for further study. To illuminate the effects of the plant extract, different concentrations (5, 10, 15, and 20 mL) were used by keeping the source of magnesium at constant level.

4.4. General procedure for the synthesis of N^{α}-protected formamides (3a-o)

A stirred solution of N^{α}-protected amino acid (1.0 mmol) in THF was cooled to −10 to −15°C and, then, NMM (1.5 mmol) and ECF (1.5 mmol) were added [44,45,54]. The reaction mixtutre was stirred for 15 minutes. Sodium azide in a minimum amount of water (2.0 mmol) was added and stirring was continued for 15 minutes. THF was then removed in vacuum and the residue was dissolved in DCM. The organic extract was washed with 10% HCl, 10% $NaHCO_3$ solution, H_2O, saturated solution of brine, and dried over anhydrous Na_2SO_4. DCM was evaporated under reduced pressure and the residue was dissolved in 15.0 mL of toluene. The formed azide was subject to Curtius rearrangement for about 45 min under reflux condition. After the complete conversion of azide to isocyanate, toluene was removed in vacuo and the resulting isocyanate was dissolved in 15 mL of dry CH_2Cl_2. To this solution was added 96% HCO_2H (2.0 mmol) and nano MgO powder (0.5 mmol) at 0°C with stirring for 4 h when a precipitate appeared. MgO was removed by filtration and the organic layer was washed with 5% citric acid (20 mL), 5% Na_2CO_3 (20 mL), and water to get crude product of formamides; then, it was purified by the recrystallization of DMSO-water system to afford analytically pure products.

4.5. Spectral data of selected compounds

(S)-(9H-fluoren-9-yl)methyl 1-formamido-2-methylpropylcarbamate (**3a**): Yield 84%; white solid; mp 183°C; R_f (10% MeOH/$CHCl_3$): 0.32; IR (ATR, cm^{-1}): 3323.60 (NH-stre), 2925.64 (C–H, CH_3), 1693.35 (–CHO), 1658.97 (Aromatic C=C), 1106.95 (HN–CH); ^{1}H NMR (d_6-DMSO): δ 0.85-0.91 (d, J = 10.0 Hz, 6H), 3.37 (s, 1H), 4.21-4.31 (t, J = 15.0 Hz, 1H), 5.05-5.06 (d, J = 5.0 Hz, 2H), 5.66-5.69 (d, J = 15.0 Hz, 1H), 7.70-7.71 (d, J = 5.0 Hz, 2H), 7.88-7.97 (m, 8H), 8.15 (s, 1H); ^{13}C NMR (d_6-DMSO): δ 18.61, 32.21, 47.18, 61.21, 65.83, 120.58, 125.69, 127.53, 128.11, 141.20, 144.28, 144.36, 160.85 ppm; calculated mass ($C_{20}H_{22}N_2O_3$) = 338.16, observed ESI-MS m/z = 361.00 $[M+Na]^+$.

(S)-(9H-fluoren-9-yl)methyl 1-formamido-2-phenylethylcarbamate (**3b**): Yield 82%; white solid; mp 191°C; R_f (10% MeOH/$CHCl_3$): 0.29; IR (ATR, cm^{-1}): 3380.76 (NH-stre), 2948.64 (C–H), 1650.68 (–CHO), 1634.46 (Aromatic C=C), 1240.42 (HN–CH). ^{1}H NMR (d_6-DMSO): δ 3.41 (s, 2H), 4.18-4.29 (t, J = 5.0 Hz, 1H), 5.03 (s, 2H), 5.40 (s, 1H), 6.01 (br, 2H), 7.25-7.93 (m, 13H), 8.44 (s, 1H); ^{13}C NMR (d_6-DMSO): δ 40.14, 47.06, 65.94, 67.80, 120.59, 125.65, 126.0, 127.55, 128.13, 128.66, 129.67, 139.5, 141.18, 144.22, 157.1, 160.74 ppm; calculated mass ($C_{24}H_{22}N_2O_3$) = 386.163, observed ESI-MS m/z = 409.00 $[M+Na]^+$.

Benzyl formamidomethylcarbamate (**3c**): Yield 89%; white solid; mp 161°C; R_f (10% MeOH/$CHCl_3$): 0.30; IR (ATR, cm^{-1}): 3318.60 (NH-stre), 2964.75 (C–H), 1692.75 (–CHO), 1645.31 (Aromatic C=C), 1102.75 (HN–CH). ^{1}H NMR (d_6-DMSO): δ 5.01 (s, 2H), 5.40 (s, 2H), 6.63 (br, 2H), 7.34 (s, 5H), 8.52 (s, 1H); ^{13}C NMR (d_6-DMSO): δ 48.25, 65.47, 127.63, 128.29, 129.0, 137.0, 156.18, 161.04 ppm; calculated mass ($C_{10}H_{12}N_2O_3$) = 208.0848, observed ESI-MS m/z = 231.0746$[M+Na]^+$.

(S)-benzyl 1-formamido-3-(methylthio)propylcarbamate (**3d**): Yield 75%; white solid; mp 159°C; R_f (10% MeOH/$CHCl_3$): 0.30; IR (ATR, cm^{-1}): 3319.62 (NH-stre), 2977.43 (C–H, CH_3), 1693.45 (–CHO), 1647.57 (Aromatic C=C), 1108.65 (HN–CH). ^{1}H NMR (d_6-DMSO): 2.03 (s, 3H), 2.14 (m, 2H), 2.40(m, 2H), 5.00 (s, 2H), 5.15 (m, 1H), 7.20 (m, 5H), 7.95 (s, 1H), 8.09 (m, 1H), 8.20 (m, 1H); ^{13}C NMR (d_6-DMSO): 15.26, 16.20, 30.21, 59.64, 66.90, 127.70, 128.38, 137.30, 158.58, 163.22. calculated mass ($C_{13}H_{18}N_2O_2S$) = 282.1038, observed ESI-MS m/z = 305.3484 $[M+Na]^+$.

(S)-tert-butyl 1-formamidoethylcarbamate (**3e**): Yield 79%; white solid; mp 183°C; R_f (10% MeOH/$CHCl_3$): 0.31; IR (ATR, cm^{-1}): 3443.80 (NH-stre), 2978.83 (C–H, CH_3), 1677.67(–CHO), 1043.34 (HN–CH). ^{1}H NMR (d_6-DMSO): δ 1.38 (s, 9H), 2.56 (d, J = 10.0 Hz, 3H), 6.14 (br, 1H), 7.30 (br, 2H), 7.80-7.90 (s, 1H); ^{13}C NMR (d_6-DMSO): δ 21.43, 28.69, 40.92, 77.53, 156.71, 162.11 ppm; calculated mass ($C_8H_{16}N_2O_3$) = 188.1161, observed ESI-MS m/z = 211.10 $[M+Na]^+$.

(S)-(9H-fluoren-9-yl)methyl 1-formamidoethylcarbamate (**3f**): Yield 82%; white solid; mp 178°C; R_f (10% MeOH/$CHCl_3$): 0.37; IR (ATR, cm^{-1}): 3318.50 (NH-stre), 2974.75 (C–H, CH_3), 1691.59 (–CHO), 1647.77 (aromatic C=C), 1104.75 (HN–CH). ^{1}H NMR (d_6-DMSO): δ 1.26-1.30 (d, J = 15.0 Hz, 3H), 3.47 (t, J = 10.0 Hz, 1H), 4.22-4.31(d, J = 20.0 Hz, 2H), 5.35 (s, 1H), 7.89-7.97 (m, 8H) 8.02 (s, 1H), 8.10 (s, 2H); ^{13}C NMR (d_6-DMSO): δ 21.32, 47.11, 53.18, 65.89, 125.62, 125.68, 127.58, 128.15, 141.21, 144.28, 155.33, 164.78 ppm; calculated mass ($C_{18}H_{18}N_2NO_3$) = 310.1317, observed ESI-MS m/z = 333.00 $[M+Na]^+$.

(S)-(9H-fluoren-9-yl)methyl 1-formamido-3-methylbutylcarbamate (**3g**): Yield 76%; white solid; mp 156°C; R_f (10% MeOH/$CHCl_3$): 0.33; IR (ATR, cm^{-1}): 3320.60 (NH-stre), 2922.55 (C–H, CH_3), 1695.57 (–CHO), 1630.45 (Aromatic C=C), 1249.66 (HN–CH). ^{1}H NMR (d_6-DMSO): δ 0.84-0.85 (d, J = $4.0Hz$, 6H), 1.03-1.06 (t, J = 8.0 Hz, 2H), 1.34-1.60 (m, 1H), 4.18-4.32 (m, 1H), 4.82-4.86 (t, J = 8.0 Hz, 2H), 5.32-5.36 (t, J = 8.0 Hz, 1H), 7.29-7.92 (m, 8H), 8.01-8.06 (br, 2H), 8.16 (s, 1H); ^{13}C NMR (d_6-DMSO): δ 21.98, 23.88, 46.67, 46.71, 54.39, 65.21, 120.05, 125.17, 127.00, 127.58, 140.70, 143.84, 156.60, 164.34, ppm; calculated mass ($C_{21}H_{24}N_2O_3$) = 352.1787, observed ESI-MS m/z = 375.1691 $[M+Na]^+$.

(S)-(9H-fluoren-9-yl)methyl 2-formamidopyrrolidine-1-carboxylate (**3h**): Yield 75%; Gum; R_f (10% MeOH / $CHCl_3$): 0.27; IR (ATR, cm^{-1}): 3320.70 (NH-stre), 2978.80 (C–H), 1691.59 (–CHO), 1649.57 (Aromatic C=C), 1110.96 (HN–CH). ^{1}H NMR (d_6-DMSO): δ 1.70 (br, 4H), 3.28 (m, 2H), 4.10 (t, J = 12.0 Hz, 1H), 4.40 (d, J = 8.0 Hz, 2H), 5.24 (m, 1H), 7.24-7.80 (m, 8H), 7.96 (s, 1H), 8.04 (m, 1H); ^{13}C NMR (d_6-DMSO): δ 23.8, 32.0, 46.8, 64.1, 66.4, 120.0, 125.2, 127.4, 127.8, 141.5, 143.6, 155.0, 165.6 ppm; Calculated mass ($C_{20}H_{20}N_2O_3$) = 336.15, observed ESI-MS m/z = 359.25 $[M + Na]^+$.

(9H-fluoren-9-yl)methyl (1S, 2S)-1-formamido-2-methylbutylcarbamate (**3i**): Yield 86%; white solid; mp 140°C; R_f (10% MeOH/$CHCl_3$): 0.33; IR (ATR, cm^{-1}): 3320.30 (NH-stre), 2965.55 (C–H, CH_3), 1690.55 (–CHO), 1648.87 (Aromatic C=C), 1100.45 (HN–CH). ^{1}H NMR (d_6-DMSO): δ 1.08 (br, 3H), 1.38 (s, 3H), 1.64 (s, 2H), 2.30 (m, 1H), 4.30-4.32 (t, J = 10.0 Hz, 1H), 4.47 (s, 2H), 5.17-5.19 (s, 1H), 7.32-7.88 (m, 8H), 8.05 (br, 2H) 8.13 (s, 1H); ^{13}C NMR (d_6-DMSO): δ 11.40, 14.81, 25.18, 39.99, 47.20, 59.63, 65.80, 125.71, 127.53, 128.11, 129.41, 141.21, 144.28, 144.37, 160.88 ppm; calculated mass ($C_{21}H_{24}N_2O_3$) = 352.1787, observed ESI-MS m/z = 375.00 $[M + Na]^+$.

(S)-(9H-fluoren-9-yl)methyl 1-formamido-2-(1H-indol-3-yl)ethylcarbamate (**3j**): Yield 87%; white solid; mp 178°C; R_f (10% MeOH/$CHCl_3$): 0.34; IR (ATR, cm^{-1}): 3379.55 (NH-stre), 2956.64 (C–H), 1654.48 (–CHO), 1636.66 (Aromatic C=C), 1238.62 (HN–CH). ^{1}H NMR (d_6-DMSO): δ 2.48-2.52 (d, J = 4.0 Hz, 2H), 4.06-4.20 (m, 1H), 5.47-5.50 (t, J = 4.0 Hz, 2H), 6.10 (t, J = 8.0 Hz, 1H), 6.97 (s, 1H), 7.19-7.67 (m, 12H), 7.95 (m, 1H), 10.80 (br, 3H); ^{13}C NMR (d_6-DMSO): δ 30.35, 46.71, 61.11, 66.98, 111.33, 118.38, 120.06, 120.88, 123.56, 125.20, 127.03, 127.28, 127.55, 127.58, 128.80, 136.05, 140.65, 143.71, 156.59, 160.35 ppm; calculated mass ($C_{26}H_{23}N_3O_3$) = 425.1739, observed ESI-MS m/z = 448.16266 $[M+Na]^+$.

(S)-benzyl 1-formamido-2-hydroxyethylcarbamate (**3k**): Yield 75%; white solid; mp 178°C; R_f (10% MeOH/$CHCl_3$): 0.33; IR (ATR, cm^{-1}): 3381.46 (NH-stre), 2947.34 (C–H), 1650.88 (–CHO), 1644.56 (Aromatic C=C), 1241.62 (HN–CH). ^{1}H NMR (d_6-DMSO): δ 2.50 (s, 1H), 3.99-4.15 (m, 2H), 5.06 (s, 2H), 5.86 (s, 1H), 7.35 (s, 5H), 7.98 (s, 1H), 8.44 (br, 2H); ^{13}C NMR (d_6-DMSO): δ 62.87, 66.08, 68.30, 128.24, 128.42, 128.86, 137.14, 155.18, 161.25 ppm; calculated mass ($C_{11}H_{14}N_2O_4$) =238.0954, observed ESI-MS m/z = 261.10 $[M+Na]^+$.

(S)-tert-butyl 1-formamido-2-phenylethyl- carbamate (**3l**): Yield 78%; white solid; mp 178°C; R_f (10% MeOH /$CHCl_3$): 0.35; IR (ATR, cm^{-1}): 3378.46 (NH-stre), 2947.64 (C–H), 1653.38 (–CHO), 1638.58 (Aromatic C=C), 1235.49 (HN–CH). ^{1}H NMR (d_6-DMSO): δ 1.32-1.35 (s, 9H), 2.78-2.94 (m, 2H), 5.30-5.38 (m, 1H), 7.16-7.36 (m, 5H), 7.59-7.60 (br, 2H), 7.88 (s, 1H); ^{13}C NMR (d_6-DMSO): δ 28.15, 40.12, 61.39, 80.29, 126.20, 128.10, 129.13, 137.38, 154.28, 164.11 ppm; calculated mass ($C_{11}H_{14}N_2O_4$) =238.1474, observed ESI-MS m/z = 261.10 $[M+Na]^+$.

Benzyl (1S, 2S)-1-formamido-2-methylbutyl- carbamate (**3m**): Yield 77%; white solid; mp 147°C; R_f (10% MeOH/$CHCl_3$): 0.30; IR (ATR, cm^{-1}): 3381.88 (NH-stre), 2947.24 (C–H, -CH_3), 1660.28 (–CHO), 1635.76 (Aromatic C=C), 1244.52 (HN–CH). ^{1}HNMR (d_6-DMSO): δ 0.82 (m, 6H), 1.01-1.84 (m, 3H), 4.99 (s, 2H), 5.16 (m, 1H), 7.26 (m, 5H), 7.92 (s, 1H),8.10 (br, 1H), 8.21 (br, 1H); ^{13}C NMR (d_6-DMSO): 10.98, 14.36, 24.76, 38.89, 59.22, 65.41, 127.73,128.34, 137.30, 160.51, 164.64 ppm; calculated mass ($C_{14}H_{20}N_2O_3$) = 264.1474, observed ESI-MS m/z = 287.1471 $[M+Na]^+$.

Tert-butyl 1-formamido-2-hydroxypropyl- carbamate (**3n**): Yield 80%; white solid; mp 177°C; R_f (10% MeOH /$CHCl_3$): 0.35; IR (ATR, cm^{-1}): 3372.48 (NH-stre), 2948.66 (C–H, CH_3), 1654.34 (–CHO), 1237.44

(HN–CH). ^{1}H NMR (d_6-DMSO): δ 1.30-1.36 (s, 9H), 1.30 (d, J = 8.0 Hz, 3H), 4.40 (m, 1H), 4.60 (d, J = 10.0 Hz, 1H), 5.60 (br, 3H), 8.20 (s, 1H); ^{13}C NMR (d_6-DMSO): δ 20.0, 28.50, 63.50, 67.80, 80.40, 156.0, 168.10 ppm; calculated mass ($C_9H_{18}N_2O_4$) =218.13, observed ESI-MS m/z = 241.23 [M+Na]$^+$.

(S)-benzyl 1-formamido-2-phenylethylcarbamate (**3o**): Yield 92%; white solid; mp 175°C; R_f (10% MeOH/$CHCl_3$): 0.30; IR (ATR, cm^{-1}): 3375.68 (NH-stre), 2948.24 (C–H), 1660.28 (–CHO), 1635.76 (Aromatic C=C), 1244.52 (HN–CH). ^{1}H NMR (d_6-DMSO): δ 2.92 (d, 2H, J = 7.2 Hz) 4.96 (s, 2H), 5.63 (m, 1H), 7.01-7.54 (m, 10H) 7.95 (s, 1H), 8.01 (m, 1H), 8.21 (m, 1H); ^{13}C NMR (d_6-DMSO): 37.41, 54.61, 66.64, 126.15, 126.30, 127.90, 128.40, 128.41, 131.56, 137.50, 159.80, 164.06 ppm; calculated mass ($C_{17}H_{18}N_2O_3$) = 298.13, observed ESI-MS m/z = 321.25 [M+Na]$^+$.

Acknowledgement

The authors thank the Principal and Director of Siddaganga Institute of Technology, Tumakuru, Karnataka, for the research facilities. One of the authors (H.S. Lalithamba) is thankful to the Vision Group of Science and Technology, Departments of Information Technology, Biotechnology, and Science & Technology, Government of Karnataka, for providing funds under CISEE programme (VGST-GRD No. 472) to carry out the present research work by means of a sponsored project. She is also thankful to the Department of Science and Technology, Government of India, for the instrumental facilities under Nano mission project.

References

1. Albadi, J., Razeghi, A., Abbaszadeh, H. and Mansournezhad, A. "Efficient Approach for the Synthesis of 2 H-indazolo [2,1-b] phthalazine-triones Catalyzed by CuO-ZnO Nanocatalyst in water", *Jordan J. Chem.*, **10**, pp. 130-136 (2015).
2. Dehghan, A. and Shams, N. "MgO nanoparticles catalyzed simple and efficient synthesis of benzylamino coumarine derivatives under in aqueous media", *Ind. J. Fundamental and Appl. Life Sciences.*, **5**, pp. 5288-5293 (2015).
3. Chaturvedi, S., Dave, P.N. and Shah, N.K. "Applications of nano-catalyst in new era", *J. Saudi Chem. Soc.*, **16**, pp. 307-325 (2012).
4. Maliyekkal, S.M., Antony, K.R. and Pradeep, T. "High yield combustion synthesis of nanomagnesia and its application for fluoride removal", *Science of the Total Envir.*, **408**, pp. 2273-2282 (2010).
5. Di, D.R., He, Z.Z., Sun, Z.Q. and Liu, J. "A new nano-cryosurgical modality for tumor treatment using biodegradable MgO nanoparticles", *Nanomed. Nanotech. Bio. and Medi.*, **8**, pp. 1233-1241 (2012).
6. Ouraipryvan, P., Sreethawong, T. and Chavadej, S. "Synthesis of crystalline MgO nanoparticle with mesoporous-assembled structure via a surfactant-modified sol-gel process", *Mater. Lett.*, **63**(21), pp. 1862-1865 (2009).
7. Mirzaei, H. and Davoodnia, A. "Microwave assisted sol-gel synthesis of MgO nanoparticles and their catalytic activity in the synthesis of hantzsch 1,4-dihydropyridines", *Chinese J. Catal.*, **33**(9), pp. 1502-1507 (2012).
8. Veldurthi, S., Shin, C.H., Joo, O.S. and Jung, K.D. "Synthesis of mesoporous MgO single crystals without templates", *Microporous Mesoporous Mat.*, **152**, pp. 31-36 (2012).
9. Zhao, Z., Dai, H., Du, Y., Deng, J., Zhang, L. and Shi, F. "Solvo- or hydrothermal fabrication and excellent carbon dioxide adsorption behaviors of magnesium oxides with multiple morphologies and porous structures", *Mat. Chem. Phys.*, **128**, pp. 348-356 (2011).
10. Alavi, M.A. and Morsali, A. "Syntheses and characterization of Mg(OH_2) and MgO nanostructures by ultrasonic method", *Ultrason. Sonochem.*, **17**, pp. 441-446 (2010).
11. Al-Gaashani, R., Radiman, S., Al-Douri, Y., Tabet, N. and Daud, A.R. "Investigation of the optical properties of $Mg(OH)_2$ and MgO nanostructures obtained by microwave-assisted methods", *J. Alloys Compounds.*, **521**, pp. 71-76 (2012).
12. Nusheh, M., Yoozbashizadeh, H., Askari, M., Kobatake, H. and Fukuyama, H. "Mechanically activated synthesis of single crystalline MgO nanostructures", *J. Alloys and Compounds.*, **506**, pp. 715-720 (2010).
13. Sun, R.Q., Sun, L.B., Chun, Y., Xu, Q.H. and Wu, H. "Synthesizing nanocrystal-assembled mesoporous magnesium oxide using cotton fibres as exotemplate", *Microporous Mesoporous Matl.*, **111**, pp. 314-322 (2008).
14. Sastry, M., Shankar, S.S., Rai, A. and Ahmad, A. "Rapid synthesis of Au, Ag, and bimetallic Au core-Ag shell nanoparticles using Neem (Azadirachta indica) leaf broth", *J. Colloid Interface Science.*, **275**, pp. 496-502 (2004).
15. Gardea-Torresdey, J.L., Parsons, J.G., Gornez, E., Videa, J., Troiani, H.E. and Santiagol, P. "Formation and growth of Au nanoparticles inside live alfalfa plants", *Nano Lett.*, **2**, pp. 397-401 (2002).
16. Jain, D., Daima, H.K., Kachhwaha, S. and Kothari, S.L. "Synthesis of plant-mediated silver nanoparticles using papaya fruit extract and evaluation of their anti-microbial activities", *Digest J. Nanomat. and Biostr.*, **4**, pp. 557-563 (2009).
17. Begum, N.A., Mondal, S., Basu, S., Laskar, R.A. and Mandal, D. "Biogenic synthesis of Au and Ag nanoparticles using aqueous solutions of black tea leaf extracts", *Colloids and Surfaces B: Biointer.*, **71**, pp. 113-118 (2009).

18. Ankamwar, B., Chaudhary, M. and Murali, S. "Gold nanotriangles biologically synthesized using tamarind leaf extract and potential application in vapor sensing", *Nano-Metal Chem.*, **35**, pp. 19-26 (2005).
19. Naveen, G.P.A.N. and Krishnakumar, G. "Traditional and medicinal uses of garcinia gummi-gutta fruit- a review", *Species.*, **4**(10), pp. 4-5 (2013).
20. Rajendran, P.C. and Nair, M.V. "Breaking seed dormancy and genderwise dimorphic differentiation in garcinia gummi-gutta var. gummigutta (L.) Rob", *Asian J. Biosci.*, **4**(1), pp. 93-99 (2009).
21. Dhanya, P. and Benny, P.J. "Larvicidal action of garcinia gummi-gutta.robs. var. gummi-gutta on dengue victim aedes aegypti", *Ind. J. Appl. Res.*, **4**, pp. 21-22 (2014).
22. Green, T.W. and Wuts, P.G.M. "Greene's protective groups in organic synthesis", 4th Edn., pp. 1110, A John Wiley & Sons, Inc publication, Wiley-Intersciences, New Jersey (1999).
23. Sheehan, H.C. and Yang, D.D.H. "The use of N-formylamino acids in peptide synthesis", *J.A.C.S.*, **80**, pp. 1154-1158 (1958).
24. Schley, N.D., Dobereiner, G.E. and Crabtree, R.H. "Oxidative synthesis of amides and pyrroles via dehydrogenative alcohol oxidation by ruthenium diphosphine diamine complexes", *Organometallics.*, **30**, pp. 4174-4179 (2011).
25. Petit, G.R., Kalnins, M.V., Liu, T.M.H., Thomas, E.G. and Parent, K. "Notes- potential cancerocidal agents. III. formanilides", *J. Org. Chem.*, **26**, pp. 2563-2566 (1961).
26. Chen, B.C., Bendarz, M.S., Zhao, R., Sundeen, J.E., Chen, P., Shen, Z., Skoumbourdis, A.P. and Barrish, J.C. "A new facile method for the synthesis of 1-arylimidazole-5-carboxylates", *Tetrahedron Lett.*, **41**, pp. 5453-5456 (2000).
27. Han, Y. and Cai, L. "An efficient and convenient synthesis of formamidines", *Tetrahedron Lett.*, **38**, p. 5423 (1997).
28. Effenberger, F. and Eichhorn, J. "Stereoselective synthesis of thienyl and furyl analogues of ephedrine", *Tetrahedron: Asymmetry.*, **8**, p. 469 (1997).
29. Ugi, I. "From isocyanides via four-component condensations to antibiotic syntheses", *Angew. Chem. Int. Ed.*, **21**, pp. 810-819 (1982).
30. Schollkopf, U. "Recent applications of α-metalated isocyanides in organic synthesis", *Angew. Chem. Int. Ed.*, **16**, pp. 339-348 (1977).
31. Kobayashi, S. and Nishio, K. "Facile and highly stereoselective synthesis of homoallylic alcohols using organosilicon intermediates", *J. Org. Chem.*, **56**, pp. 6620-6628 (1994).
32. Kim, S.J., Jeon, H., Oh, S.J., Lee, S.S., Choi, Y., Park, J.S. and Jeong, S. "Formamide mediated, air-brush printable, indium-free soluble Zn-Sn-O semiconductors for thin-film transistor applications", *ACS Appl. Mater. Interfaces*, **6**, pp. 18429-18434 (2014).
33. Sudarshan, N.S., Narendra, N., Hemantha, H.P. and Sureshbabu, V.V. "An efficient conversion of the carboxylic group of N-Fmoc alpha-amino acids/peptide acids into N-formamides employing isocyanates as key intermediates", *J. Org. Chem.*, **72**, pp. 9804-9807 (2007).
34. Lei, M., Ma. L. and Hu. L. "A convenient one-pot synthesis of formamide derivatives using thiamine hydrochloride as a novel catalyst", *Tetrahedron Lett.*, **51**, pp. 4186-4188 (2010).
35. Blicke, F.F. and Lu, C.J.J. "Formylation of amines with chloral and reduction of the N-formyl derivatives with lithium aluminum hydride", *J.A.C.S.*, **74**, pp. 3933-3934 (1952).
36. Suchy, M., Elmehriki, A.A.H. and Hudson, R.H.E. "Transamidation of primary amides with amines catalyzed by zirconocene dichloride", *Organic Lett.*, **13**, pp. 3952-3955 (2011).
37. Hosseni-Sarvari, M. and Sharghi, H.J. "ZnO as a new catalyst for N-formylation of amines under solvent-free conditions", *J. Org. Chem.*, **71**, pp. 6652-6654 (2006).
38. Joong-Gon, K. and Doo Ok, Jang. "Solvent-free Zinc-catalyzed amine N-formylation", *Bull. Korean Chem. Soc.*, **31**, pp. 2989-2991 (2010).
39. Saidi, O., Mark, J.B., Andrew, J.B., James, L., Stephen, P.M., Pawel, P., Robert, J.W. and Jonathan, M.J.W. "Iridium-catalyzed formylation of amines with paraformaldehyde", *Tetrahedron Lett.*, **51**, pp. 5804-5806 (2010).
40. Hao, L., Zhao, Y., Yu, B., Yang, Z., Zhang, H., Han, B., Gao, X. and Liu, Z. "Imidazolium-based ionic liquids catalyzed formylation of amines using carbon dioxide and phenylsilane at room temperature", *ACS Catal.*, **5**, pp. 4989-4993 (2015).
41. Sajadi, S.M., Maham, M. and Rezaei, A. "An eco-friendly N-formylation of amines using nano cerium oxide as a recyclable catalyst under solvent-free and ultrasound irradiation conditions at room temperature", *Lett. in Org. Chem.*, **11**, pp. 49-54 (2014).
42. Hosseini-Sarvari, M., Sodagar, E. and Doroodmandt, M.M. "Nano sulfated titania as solid acid catalyst in direct synthesis of fatty acid amides", *J. Org. Chem.*, **76**, pp. 2853-2859 (2011).
43. Sadeghpour, M., Olyaei, A., Derikvand, Z., Razeghi, R. and Vaziri, M. "Zr-MCM-41 nano reactors: a highly efficient, reusable and novel catalyst for the synthesis of N-heteroaryl formamides under solvent-free conditions", *J. Basic Appl. Science Res.*, **3**, pp. 125-128 (2013).
44. Patil, B.S., Ramu, Vasanthakumar, G.R. and Suresh Babu, V.V. "Isocyanates of N^{α}-[(9-fluorenylmethyl) oxy] carbonyl amino acids: synthesis, isolation, characterization, and application to the efficient synthesis of urea peptidomimetics", *J. Org. Chem.*, **68**, pp. 7274-7280 (2003).
45. Sureshbabu, V.V. and Narendra, N. "Synthesis of N-Z, N^{α}-formyl α-amino acid derived gem-diamines", *Int. J. Pept. Res. Ther.*, **14**, pp. 201-207 (2008).

46. Tamizh, S.K., Rathnakumari. M., Priya. M. and Suresh Kumar, P. "Shape transition effect of temperature on MgO nanostructures and its optical properties", *Int. J. Scientific & Engg. Res.*, **5**, pp. 60-64 (2014).

47. Rao, C.N.R., *Chemical Applications of Infrared and Raman Spectroscopy*, 1st Edn., p. 683, Academic Press, New York and London (1963).

48. Zong, Y., Bice, T.W., Ton-That, H., Schneewind, O. and Narayana, S.V. "Crystal structures of Staphylococcus aureus sortase A and its substrate complex", *J. Biol. Chem.*, **279**, pp. 31383-31389 (2004).

49. Isupov, M.N., Obmolova, G., Butterworth, S., Badet-Denisot, M.A., Badet, B., Polikarpov, I., Littlechild, J.A. and Teplyakov, A. "Substrate binding is required for assembly of the active conformation of the catalytic site in Ntn amido transferases: evidence from the 1.8 $\mathring{a}$ crystal structure of the glutaminase domain of glucosamine 6-phosphate synthase", *Structure.*, **4**, pp. 801-810 (1996).

50. Roman, A., Laskowski and Swindells, M.B. "LigPlot^{+}: multiple ligand-protein interaction diagrams for drug discovery", *J. Chem. Inf. Model.*, **51**, pp. 2778-2786 (2011).

51. Uma, K., Lalithamba, H.S., Raghavendra, M., Chandramohan, V. and Anupama, C. "Synthesis of N^{α}-protected aminoacid/peptide Weinreb amides employing N, N'-carbonyldiimidazole as activating agent; studies on docking and antibacterial activities", *Arkivoc.*, **4**, pp. 339-351 (2016).

52. Lingaraju, K., Raja Naika, H., Manjunath, K., Basavaraj, R.B., Nagabhushana, H., Nagaraju, G. and Suresh, D. "Biogenic synthesis of zinc oxide nanoparticles using Ruta graveolens (L.) and their antibacterial and antioxidant activities", *Appl. Nanoscience.*, **1**, pp. 1-8 (2015).

53. Ganapathi, R.K., Ashok, C.H., Venkateswara, R.C.H., Shilpa. C.C.H. and Akshaykranth, A. "Eco-friendly synthesis of MgO nanoparticles from orange fruit waste", *Int. J. Adv. Res. in Phy. Science.*, **2**, pp. 1-6 (2015).

54. Sureshbabu, V.V., Narendra, N. and Kantharaju. "Pentafluorophenyl (tertbutoxycarbonylamino)methyl carbamates: Synthesis, isolation and application to the synthesis of ureidopeptides", *Ind. J. Chem.*, **47B**, pp. 920-926 (2008).

Biographies

Mahadevaiah Raghavendra was born in India in 1989 and is a PhD research scholar working under the supervision of Dr. H.S. Lalithamba. He received his BSc and MSc degrees in Chemistry from the Tumkur University, Tumakuru and Davangere University, Davangere, in 2010 and 2012, respectively. His research interests include nano metal oxide, and peptides and peptidomimetics. All the synthesized compounds presented in this research paper were prepared by him under the supervision of Dr. H.S. Lalithamba.

Haraluru Shankaraiah Lalithamba was born in India in 1973. She received her BSc and MSc degrees in Chemistry and Organic Chemistry from the Bangalore University, Bangalore, India, in 1994 and 1996, respectively, and her PhD degree in peptides and peptidomimetics from Bangalore University, Bangalore, India, in 2012. She is currently Associate Professor in the Department of Chemistry, Tumakuru, India. Her research interests include synthesis of biologically active peptides and peptidomimetics, biological activity, molecular docking, and nano metal oxides. She actively participates in VGST, Government of Karnataka funded research projects for the synthesis of bioactive peptides and peptidomimetics. She has published more than 10 scientific research articles in reputed journals, which have been cited by other researchers.

Belenahalli Shekarappa Sharath was born in India in 1991 and is a PhD Research Scholar working under the supervision of Dr. Manjunatha Hanumanthappa. He received his BSc and MSc degrees in Biotechnology from the Kuvempu University, Shimoga, in 2012 and 2014, respectively. His research interests include Protein-Protein Interaction Network (PPIN), pathway network construction and its analysis, molecular simulation studies, and various aspects of biology systems. All the compounds in the molecular docking work were prepared by him.

Hanumanaika Rajanaika was born in India in 1980. He received his BSc and MSc degrees in Biotechnology from the Kuvempu University, Shimoga, in 2002 and 2004, respectively, and his PhD degree in Pharmacological Activities of Clematisgouriana Roxb and Naravelia Zeylanica from Kuvempu University, Shimoga, India, in 2009. He is currently working as Assistant Professor in the Department of Biotechnology, Tumakuru University, Tumakuru, India. His research interests include plant biotechnology, virology, and pharmacology. The antibacterial activity of synthesized compounds was carried out under his supervision.